

Generation of classical non-Gaussian distributions by squeezing a thermal state into non-linear motion of levitated optomechanics

R. Muffato,^{1,2} T. Georgescu,¹ J. Homans,¹ T. Guerreiro,² Q. Wu,³
D. Chisholm,³ M. Carlesso,^{4,5,3} M. Paternostro,^{6,3} and H. Ulbricht^{1,*}

¹*School of Physics and Astronomy, University of Southampton, SO17 1BJ, Southampton, England, UK*

²*Department of Physics, Pontifical Catholic University of Rio de Janeiro, Brazil*

³*Centre for Quantum Materials and Technologies, School of Mathematics and Physics, Queen's University Belfast, BT7 1NN, United Kingdom*

⁴*Department of Physics, University of Trieste, Strada Costiera 11, 34151 Trieste, Italy*

⁵*Istituto Nazionale di Fisica Nucleare, Trieste Section, Via Valerio 2, 34127 Trieste, Italy*

⁶*Università degli Studi di Palermo, Dipartimento di Fisica e Chimica - Emilio Segrè, via Archirafi 36, I-90123 Palermo, Italy*

(Dated: January 9, 2024)

We report on an experiment achieving the dynamical generation of non-Gaussian states of motion of a levitated optomechanical system. We access intrinsic Duffing-like non-linearities by squeezing an oscillator's state of motion through rapidly switching the frequency of its trap. We characterize the experimental non-Gaussian state against expectations from simulations and give prospects for the emergence of genuine non-classical features.

Introduction – Macroscopic quantum states are regarded as ideal platforms to test for the existence of intrinsic limitations in quantum formalism [1] and the effects of gravity in quantum systems [2]. While various platforms have been considered for generating such states [3], levitated systems have emerged as a front-runner in light of the possibility to achieve remarkable environmental isolation [4] and embed control techniques in their dynamics. Engineering non-classical states of levitated mechanical systems is achieved by inducing non-linear dynamics to sufficiently coherent initial states of motion [5, 6]. Accessing non-linearity by motional squeezing – sometimes assisted by a dark trap – can be instrumental to preparing non-classical states [7]. The fundamental building block of such operations, namely the squeezing of thermal states of motion of levitated particles, has been demonstrated by rapid (i.e. faster than the oscillation frequency) switching between different trap frequencies [8] or using cavities [9, 10]. Such switches can be treated as pulses applied to the particle's spring constant and have been used to drive a classical harmonic oscillator [11]. Repeated gentle squeezing pulses applied to the thermal motional state's momentum can increase the particle's oscillation amplitude, allowing it to explore the non-linear flat extremities of the trapping potential while remaining trapped. Correspondingly, the dynamics can pick up Duffing-like non-linearities, as already demonstrated [12].

In this paper, we experimentally demonstrate how a sequence of repeated pulses can be used to dynamically produce a significantly non-Gaussian state of motion by accessing intrinsic trapping-potential non-linearities and controlling their effects. We show the time-trace, in phase space, of the motional state resulting from the application of our protocol to an initial thermal state, demonstrating the emergence of non-trivial transient bimodal distributions whose relaxation dynamics we character-

ize experimentally. Moreover, we provide a quantitative perspective for the emergence of genuine quantum features of motion from a sufficiently coherent initial state of the particle [13–17]. We show how this would result in negative phase-space distributions, thus unambiguously demonstrating non-classicality, reminiscent of Schrödinger cat-like states of significant relevance for quantum information processing and fundamental tests of quantum mechanics.

Theoretical model – We refer to the setting illustrated in Fig 1A, which depicts a nanoparticle trapped in an optical tweezer in vacuum. In general, the particle motion occurs in all three spatial directions (x, y, z), while possibly involving rotational motion as well. However, in our experimental setup, we have been able to ascertain the quasi-one-dimensional nature of the oscillatory motion of our particle (which we will assume takes place along the x axis), with the remaining spatial degrees of freedom being irrelevant to the dynamics. We model the stochastically driven and damped oscillatory motion of a levitated particle in a vacuum by a one-dimensional Langevin-type equation for the time-dependent position $x(t)$ of the centre-of-mass motion of the particle of mass m in the trap

$$\ddot{x}(t) = -\Gamma_m \dot{x}(t) + S(t) \frac{F(x)}{m} + \frac{\mathcal{F}_{fluct}(t)}{m}, \quad (1)$$

where, in the regime dominated by the background gas pressure P , the damping rate can be written as [18]

$$\Gamma_m = \frac{64r^2P}{m_{gas}\bar{v}_{gas}}, \quad (2)$$

with m_{gas} and \bar{v}_{gas} the mass and mean thermal velocity of the gas molecules at room temperature, while r is the radius of the trapped silica particle. The second term in the right-hand side of Eq. (1) is the position-dependent

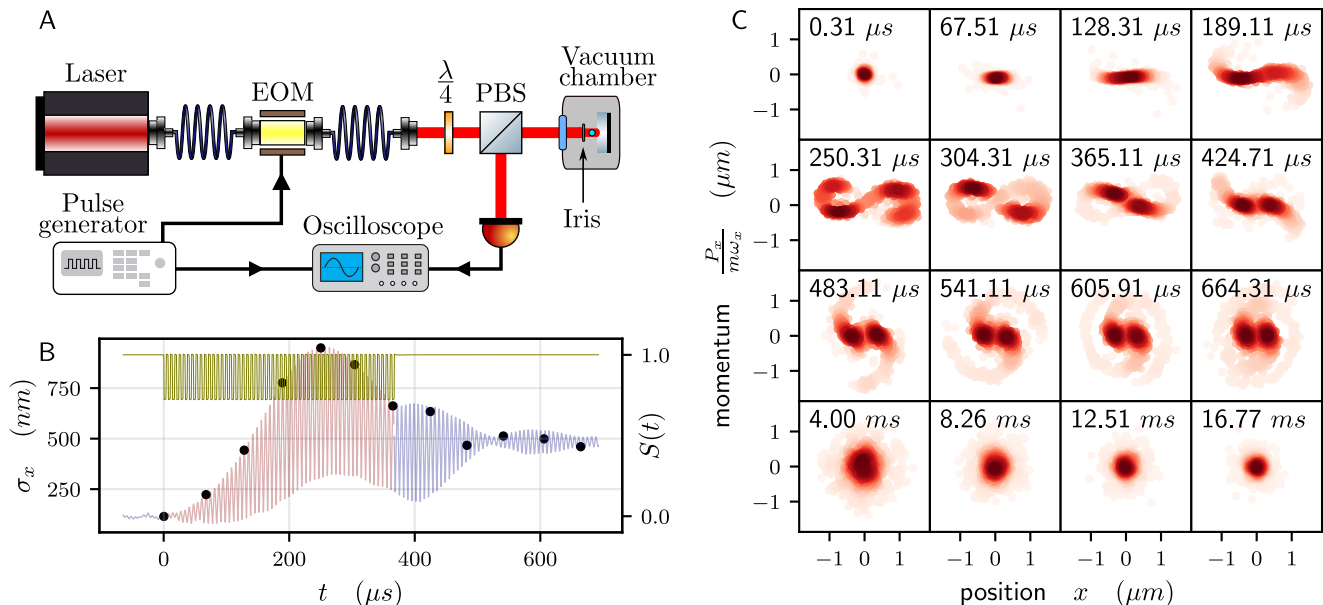


FIG. 1. Panel A: Schematic of experimental setup. A silica nanoparticle is trapped by an optical tweezers in vacuum. An electro-optical modulator (EOM) controlled by a pulse generator modulates the power of the laser. The oscilloscope receives the signal from the particle. Its acquisition is triggered by a synchronous signal from a pulse generator. Panel B: Experimental time evolution of the standard deviation of the particle position as measured by the photodiode (Blue/red line). Green line is the intensity modulation function $S(t)$, see Eq. (1), applied to the trapping laser beam via the EOM. Panel C: Experimental time-trace of the phase-space distribution of an initial thermal state of motion of the particle subjected to our protocol. Snapshots of distribution are indicated as black dots in panel B.

restoring force originating from the interaction with a Gaussian light beam in the Rayleigh regime. In the large oscillation-amplitude limit, this force is given by

$$F(x) = \frac{2\pi n_m r^3}{c} \left(\frac{n_r^2 - 1}{n_r^2 + 2} \right) \frac{\partial I}{\partial x}, \quad (3)$$

with n_m and n_p being the refractive index of the medium and of the silica particle (here assumed to take the nominal values of 1 and 1.44, respectively), $n_r = n_p/n_m$ the relative refractive index, c the speed of light, and I the intensity of the trapping laser beam. Eq. (3) gives rise to a nonlinear force directed along the gradient of the optical potential $U(x)$ such that $F(x) = -\partial_x U(x)$ [19–21], which we control by modulating in time the power of the trapping laser according to the function $S(t)$ in Eq. (1) and as illustrated in Fig. 1B [8]. The last term in the right-hand side of Eq. (1) describes the driving of the harmonic motion by random background gas collisions, which are modelled as the time-dependent stochastic force $\mathcal{F}_{fluct}(t) = \sqrt{2\Gamma_m k_B T} \eta(t)$. Here, k_B is the Boltzmann's constant and T the temperature of the gas surrounding the oscillating particle [22], while $\eta(t)$ is a zero-mean, delta-correlated Gaussian white noise such that $\langle \eta(t)\eta(t') \rangle = \delta(t - t')$. We have integrated Eq. (1) numerically using the Euler-Maruyama method [23] and sampling the initial values of position and momentum of the particle from a thermal state. The results of our

analysis are shown as the phase-space probability distributions in Fig. 2A-C.

Experiment – The experimental setup is illustrated in Fig. 1A. We use a parabolic mirror to focus light at the wavelength of 1550 nm to a diffraction-limited spot of the diameter of $1\mu\text{m}$. A pulse generator (Berkeley BNC 525) and an electro-optical modulator (EOM, Jenoptik AM1550b) are used to modulate the laser intensity as a square-wave with high and low levels of 80 mW and 57 mW respectively, to trap a silica particle of close to spherical shape (450 nm diameter) from a spray in the focal point. We monitor the centre-of-mass motion of the trapped particle by detecting a small fraction of Rayleigh back-scattered light from the trapping field with a single photodiode detector (see Ref. [24] for technical details). An iris is mounted on top of the parabola to suppress unwanted light reflected from the flat edges of the mirror and make sure that all the detected signal comes from the particle only. This guarantees the reliable assessment of the particle's center-of-mass position with only negligible distortions. Calibration of motional amplitudes and the mass of the trapped particle was done assuming perfect equilibrium of the particle with the background gas at 5 mbar by fitting a Lorentzian to the trap frequency peak [24].

To prepare bimodal states of motion the pressure is further reduced to 1×10^{-2} mbar and the particle reso-

nance frequency $\omega/2\pi = 77$ kHz is evaluated from the spectrum of the signal at the high-power level. Each pulse is timed so that the particle completes a quarter of an oscillation at each power level corresponding to $\tau_{high} = 2\omega/\pi = 3.25 \mu\text{s}$ and of $\tau_{low} = 2\omega/\sqrt{S}\pi = 3.48 \mu\text{s}$ at the high and low power level respectively. One pulse sequence consists of a train of 55 pulses as constructed on the pulse generator to prepare the bimodal state. Data acquisition by the oscilloscope was synchronised with the pulse generator and 689 pulse sequences are acquired with 518 ms between successive sequences which is about 25 times longer than the extracted 20 ms relaxation time, in good agreement with Eq.(2), allowing the particle to relax back to the thermal state between consecutive runs.

Results and Discussion – The trap non-linearity generating the non-Gaussian state is small in typical experimental conditions [18]. Taylor expansion of the gradient force up to third order shows that the Duffing parameter is proportional to the beam’s waist. Considering it as a measure for the range of nonlinearity, we note that it is larger than the spread of the thermal state $\sigma_{thermal} = \sqrt{k_B T/k}$, where k is the optomechanical spring constant and T the motional temperature. This means that the particle hardly visits the nonlinear part

of the potential. By squashing the motional state, we induce sufficient elongation such that the vertexes of the state are eventually extended to nonlinear parts of the potential well and the non-linear effect dominates the dynamics. In these regions, the particle’s dynamics is slower due to a softer effective spring constant making the tip of the ellipse lag behind compared to the faster harmonic behaviour near the centre. In the course of sufficiently many weak pulses, the state changes its shape, steadily transforming it from the initial circular thermal Gaussian to a squashed ellipsoidal and eventually to curved spiral where probability mass starts to accumulate, forming a multi-modal state.

To quantify the non-Gaussianity of the resulting simulated and experimentally obtained states, we adopt a non-dimensional measure of bi-modality [25],

$$A_D = \frac{\sqrt{2}}{\sigma_T} |\mu_1 - \mu_2|, \quad (4)$$

where $\mu_{1,2}$ are the positions of the peaks of the distribution and $\sigma_T = \sqrt{\sum_{i=1}^2 \sigma_i^2}$ is defined in terms of the individual peak’s variances $\sigma_{1,2}$ [cf. Fig. 2H]. By curve fitting a double Gaussian function to our experimental and simulated data we find the values of $A_D^{exp} = 3.95$ and $A_D^{sim} = 3.32$ in good agreement with 12% deviation which we identify to be originated by a small difference in the shape of the real trapping potential from the simulated one. The influence of the potential’s non-linearity is understood to be negligible in the linear section near the trap centre and to become dominating towards the asymptotically flat edges of the optical trap. Despite knowing general features of the non-linearity of the potential well, its exact profile is not experimentally known. As such, simulations assuming an ideal sharp beam profile were found to deviate more from the experimental results. We also find that the experimental thermal state has some outlier points that overextend the tails of Gaussian distribution, which are not included in the simulations and contribute to a softening of the potential and a larger value for A_D^{exp} . We explain outliers by a build-up of amplitude as a net effect from multiple collisions by background gas particles or other perturbations affecting the trap.

Quantum model – To acquire the picture of the nonlinear squeezing effect in the quantum regime, we study the protocol with the quantum model built in Refs. [26, 27]. We thus model the oscillator as a large angular-momentum system under the Holstein–Primakoff transformation [28], through which the dynamics is simulated. The model captures well all quantum effects in the low-energy sector of the Hilbert space, and has been used to assess the out-of-equilibrium thermodynamics of quantum-controlled evolution in the non-Gaussian regime [26, 27]. The results for the case study of the nonlinear squeezing protocol in the quantum regime is shown

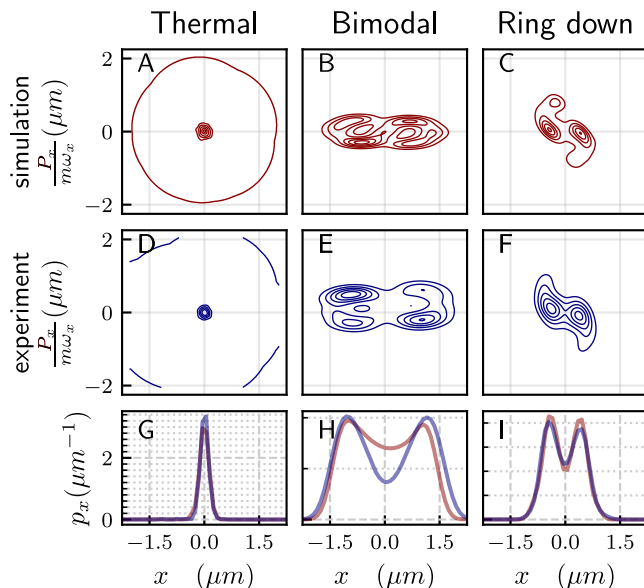


FIG. 2. Comparisons between simulations (red lines) and experimental reconstructions (blue lines) of the phase-space distributions associated with paradigmatic states of motion of the levitated particle. Panels A and D: Initial thermal state; Panels B and E: initial non-Gaussian bimodal state; Panel C and F: The initial distribution is that of the motional state achieved by stopping the dynamical protocol. Such state will eventually relax back to a thermal configuration. Panels G-I show the projection of the phase-space distribution, with p_x the position probability function for the three initial states described above.

in Fig. 3. The Hamiltonian for the quantum system is given by

$$\hat{H}_s(t) = \frac{\hat{p}_x^2}{2m} - \mathcal{E}(t)e^{-\frac{1}{2}m\omega^2\hat{x}^2}, \quad (5)$$

where \hat{x} and \hat{p}_x are the position and momentum operators. The potential of the system given by the second term is an inverted Gaussian, where $\mathcal{E}(t)$ controls the energy scale (the depth) of the potential [cf. Fig. 3A]. To implement the squeezing protocol, we modulate the energy scale of the potential every quarter of the oscillation as $\mathcal{E}(t) = \zeta(t)\mathcal{E}_0$ with

$$\zeta(t) = \begin{cases} 10, & \text{for } t' = 0 \text{ or } t' \in [t_1, t_1 + t_2], \\ 7, & \text{for } t' \in [0, t_1], \end{cases} \quad (6)$$

Here $t' = t \bmod (t_1 + t_2)$, while t_1 and t_2 are the times necessary for a quarter of oscillation for $\zeta = 7$ and $\zeta = 10$ respectively. Then, the time counter t' resets every half an oscillation. In this case study, we take the system ground state as the initial state, and evolve it following the von-Neumann master equation, $\dot{\hat{\rho}}(t) = -\frac{i}{\hbar}[\hat{H}_s(t), \hat{\rho}(t)]$. We now assume units such that $\hbar = m = \omega = \mathcal{E}_0 = 1$, thus getting $t_1 = 0.78$ and $t_2 = 0.61$, and simulate the dynamics for 5 oscillations. We show the potentials for the nonlinear squeezing protocol and the initial state respectively in Figs. 3A and 3D.

We study the system dynamics by using the Wigner distribution $\mathcal{W}_{x,p_x}(t)$. Quantum states of the system could give rise to the negativity of the Wigner function, a feature that can be used to witness non-classicality. In particular, as it is shown in Fig. 3E, the nonlinear squeezing protocol described here drives the ground state of the system to states whose Wigner function showcases significant negative values. A way to quantitatively characterize such non-classicality is the negativity $\mathcal{N}(t)$, which is defined by integrating the Wigner distribution over the region of the phase space Σ_- where it attains negative values, that is

$$\mathcal{N}(t) = \iint_{\Sigma_-} dx dp_x \mathcal{W}_{x,p_x}(t). \quad (7)$$

As the Wigner distribution is normalised, we have $|\mathcal{N}(t)| \in [0, 1]$. Fig. 3B shows the behaviour of $\mathcal{N}(t)$ for our nonlinear squeezing protocol. The negativity shows a monotonic trend during the nonlinear squeezing process, with fluctuations due to the modulation of $\mathcal{E}(t)$. Harnessing the negativity of the Wigner distribution is not a straightforward task, unless the structure of the state is known. In order to gather insight, we consider a cat-like state of the form

$$|\psi\rangle = \frac{|\alpha\rangle + |-\alpha\rangle}{\sqrt{2(1 + e^{-2|\alpha|^2})}}, \quad \alpha \in \mathbb{C}, \quad (8)$$

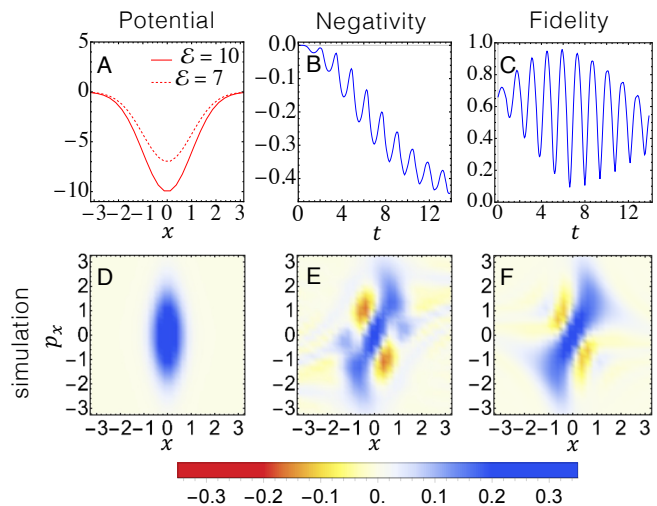


FIG. 3. Case study of the quantum nonlinear squeezing protocol. Panel A shows the potentials with different energy scale \mathcal{E} . Panel B shows the Wigner negativity $\mathcal{N}(t)$ of the system over the process. Panel C shows the maximum fidelity between the system and the cat state achieved by choosing a suitable value of α . Panels D-F show the Wigner distributions of the initial state, of the state evolved at $t = 8.69$, and of the cat state with $\alpha = 0.8 + 0.75i$ [cf. Eq. (8)], respectively.

where we choose $|\alpha| \geq 1$ so the state has clearly a non-Gaussian Wigner distribution. Such a state is a resource in a widespread range of applications, from continuous-variable quantum computing to quantum communication and the test of quantum gravity. Here, we quantify the closeness of the state produced by our squeezed protocol and a state such as the one in Eq. (8). As an instance, we consider $\alpha = 0.8 + 0.75i$, whose Wigner distribution is represented in Fig. 3F. We use the state fidelity $\mathcal{F}(t) = \langle \psi | \hat{\rho}(t) | \psi \rangle$ between such reference and the state of the nonlinear oscillator here at hand to quantify their closeness. By taking an evolution time $t = 8.69$, we achieve $\mathcal{F} = 0.886$ [cf. Figs. 3E and 3F]. By varying the amplitude α of the coherent states entering Eq. (8), such fidelity can be optimised for every state of the nonlinear oscillator, as shown in Fig. 3C, whose values oscillate and achieve an overall maximum $\mathcal{F}_{\max} = 0.949$ at $t = 4.52$.

Conclusion – We have shown experimentally that the controlled access of intrinsic trap non-linearities can be used for the generation of non-Gaussian classical states. We show theoretically that, if the motional state is initially cooled to enhance the state coherence, our scheme can be used to generate non-Gaussian states with a genuinely non-classical character, as witnessed by significantly negative Wigner distributions. Such states appear to share remarkable similarities with cat-like states, opening up the possibility for their use in protocols for quantum information processing and quantum sensing. Enhanced bimodal effects can be achieved by using stronger non-linearities, such as those from engineered

potentials [6] and deploying quantum control methods of thermodynamic inspiration [27], which will be the focus of forthcoming work. Periodically driving mechanical motion as in our squeezing protocol is also predicted to enhance force sensing capabilities of levitated mechanics [29].

Acknowledgements – We thank for discussions Jakub Wardak, Elliot Simcox, and Chris Timberlake. We acknowledge funding from the EPSRC International Quantum Technologies Network Grant *Levinet* (EP/W02683X/1). We further acknowledge financial support from the UK funding agency EPSRC (grants EP/W007444/1, EP/V035975/1, EP/V000624/1, EP/X009491/1 and EP/T028424/1), the Leverhulme Trust (RPG-2022-57 and RPG-2018-266), the Royal Society Wolfson Fellowship (RSWF/R3/183013), the Department for the Economy Northern Ireland under the US-Ireland R&D Partnership Programme, the EU Horizon 2020 FET-Open project TeQ (766900), the PNRR PE Italian National Quantum Science and Technology Institute (PE0000023) and the EU Horizon Europe EIC Pathfinder project QuCoM (GA no.10032223). We further acknowledge support from the QuantERA grant LEMAQUME, funded by the QuantERA II ERA-NET Cofund in Quantum Technologies implemented within the EU Horizon 2020 Programme.

* Correspondence email address: H.Ulbricht@soton.ac.uk;

- [1] M. Arndt and K. Hornberger, Testing the limits of quantum mechanical superpositions, *Nature Physics* **10**, 271 (2014).
- [2] D. Carney, P. C. Stamp, and J. M. Taylor, Tabletop experiments for quantum gravity: a user’s manual, *Classical and Quantum Gravity* **36**, 034001 (2019).
- [3] S. Nimmrichter and K. Hornberger, Macroscopicity of mechanical quantum superposition states, *Physical Review Letters* **110**, 160403 (2013).
- [4] C. Gonzalez-Ballester, M. Aspelmeyer, L. Novotny, R. Quidant, and O. Romero-Isart, Levitodynamics: Levitation and control of microscopic objects in vacuum, *Science* **374**, eabg3027 (2021).
- [5] M. Roda-Llodes, A. Riera-Campenya, D. Candoli, P. T. Grochowski, and O. Romero-Isart, Macroscopic quantum superpositions via dynamics in a wide double-well potential, arXiv preprint arXiv:2303.07959 (2023).
- [6] A. A. Rakhubovsky, D. W. Moore, and R. Filip, Non-classical states of levitated macroscopic objects beyond the ground state, *Quantum Science and Technology* **4**, 024006 (2019).
- [7] E. Bonvin, L. Devaud, M. Rossi, A. Militaru, L. Dania, D. S. Bykov, O. Romero-Isart, T. E. Northup, L. Novotny, and M. Frimmer, State expansion of a levitated nanoparticle in a dark harmonic potential, arXiv:2312.13111 (2023).
- [8] M. Rashid, T. Tufarelli, J. Bateman, J. Vovrosh, D. Hempston, M. Kim, and H. Ulbricht, Experimental realization of a thermal squeezed state of levitated optomechanics, *Physical Review Letters* **117**, 273601 (2016).
- [9] T. Penny, A. Pontin, and P. Barker, Sympathetic cooling and squeezing of two colevitated nanoparticles, *Physical Review Research* **5**, 013070 (2023).
- [10] Y. Li, A.-N. Xu, L.-G. Huang, and Y.-C. Liu, Mechanical squeezing via detuning-switched driving, *Physical Review A* **107**, 033508 (2023).
- [11] V. I. Arnol’d, *Mathematical methods of classical mechanics*, Vol. 60 (Springer Science & Business Media, 2013).
- [12] A. Setter, J. Vovrosh, and H. Ulbricht, Characterization of non-linearities through mechanical squeezing in levitated optomechanics, *Applied Physics Letters* **115** (2019).
- [13] F. Tebbenjohanns, M. L. Mattana, M. Rossi, M. Frimmer, and L. Novotny, Quantum control of a nanoparticle optically levitated in cryogenic free space, *Nature* **595**, 378 (2021).
- [14] U. Delić, M. Reisenbauer, K. Dare, D. Grass, V. Vuletić, N. Kiesel, and M. Aspelmeyer, Cooling of a levitated nanoparticle to the motional quantum ground state, *Science* **367**, 892 (2020).
- [15] L. Magrini, P. Rosenzweig, C. Bach, A. Deutschmann-Olek, S. G. Hofer, S. Hong, N. Kiesel, A. Kugi, and M. Aspelmeyer, Real-time optimal quantum control of mechanical motion at room temperature, *Nature* **595**, 373 (2021).
- [16] M. Kamba, R. Shimizu, and K. Aikawa, Optical cold damping of neutral nanoparticles near the ground state in an optical lattice, *Optics Express* **30**, 26716 (2022).
- [17] A. Ranfagni, K. Børkje, F. Marino, and F. Marin, Two-dimensional quantum motion of a levitated nanosphere, *Physical Review Research* **4**, 033051 (2022).
- [18] J. Gieseler, L. Novotny, and R. Quidant, Thermal nonlinearities in a nanomechanical oscillator, *Nature Physics* **9**, 806 (2013).
- [19] P. H. Jones, O. M. Maragò, and G. Volpe, *Optical tweezers: Principles and applications* (Cambridge University Press, 2015).
- [20] A. Ashkin, J. M. Dziedzic, J. E. Bjorkholm, and S. Chu, Observation of a single-beam gradient force optical trap for dielectric particles, *Optics Letters* **11**, 288 (1986).
- [21] Y. Harada and T. Asakura, Radiation forces on a dielectric sphere in the rayleigh scattering regime, *Optics communications* **124**, 529 (1996).
- [22] R. Kubo, The fluctuation-dissipation theorem, *Reports on Progress in Physics* **29**, 255 (1966).
- [23] G. Volpe and G. Volpe, Simulation of a brownian particle in an optical trap, *American Journal of Physics* **81**, 224 (2013).
- [24] J. Vovrosh, M. Rashid, D. Hempston, J. Bateman, M. Paternostro, and H. Ulbricht, Parametric feedback cooling of levitated optomechanics in a parabolic mirror trap, *JOSA B* **34**, 1421 (2017).
- [25] K. M. Ashman, C. M. Bird, and S. E. Zepf, Detecting bimodality in astronomical datasets, *Astron. J.* **108**, 2348 (1994).
- [26] Q. Wu, L. Mancino, M. Carlesso, M. A. Ciampini, L. Magrini, N. Kiesel, and M. Paternostro, Nonequilibrium quantum thermodynamics of a particle trapped in a controllable time-varying potential, *PRX Quantum* **3**, 010322 (2022).
- [27] Q. Wu, M. A. Ciampini, M. Paternostro, and M. Carlesso, Quantifying protocol efficiency: A thermodynamic figure of merit for classical and quantum state-transfer

- protocols, Phys. Rev. Res. **5**, 023117 (2023).
- [28] J. A. Gyamfi, An Introduction to the Holstein-Primakoff Transformation, with Applications in Magnetic Resonance, arXiv.1907.07122 (2019).
- [29] F. Cosco, J. Pedernales, and M. B. Plenio, Enhanced force sensitivity and entanglement in periodically driven optomechanics, Physical Review A **103**, L061501 (2021).